Electronic Supplementary Material (ESI) for RSC Advances.

The utilization of a stable 2D bilayer MOF on luminescent and photocatalytic properties simultaneously: experimental studies and theoretical analysis

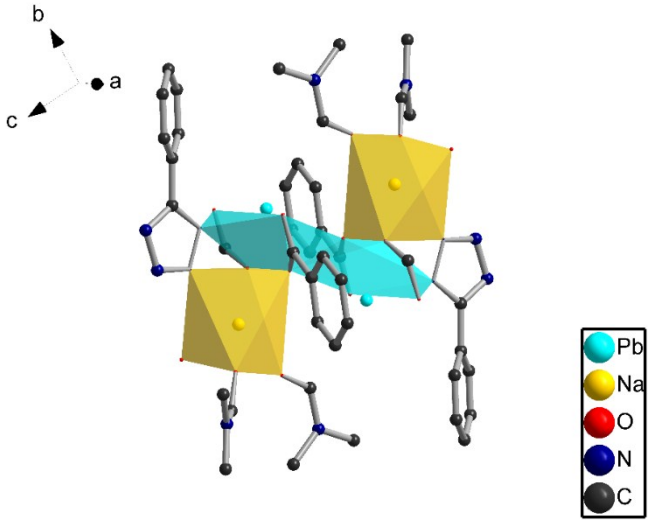

Fig. S1 view of the 4-connected cluster.

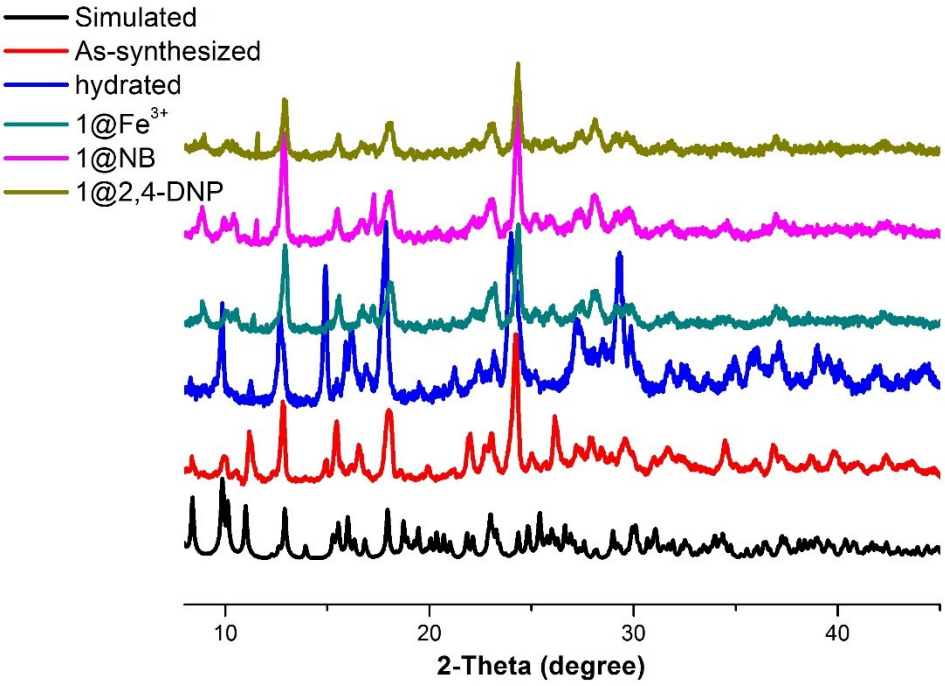

Fig. S2 view of the PXRD patterns of different systems.

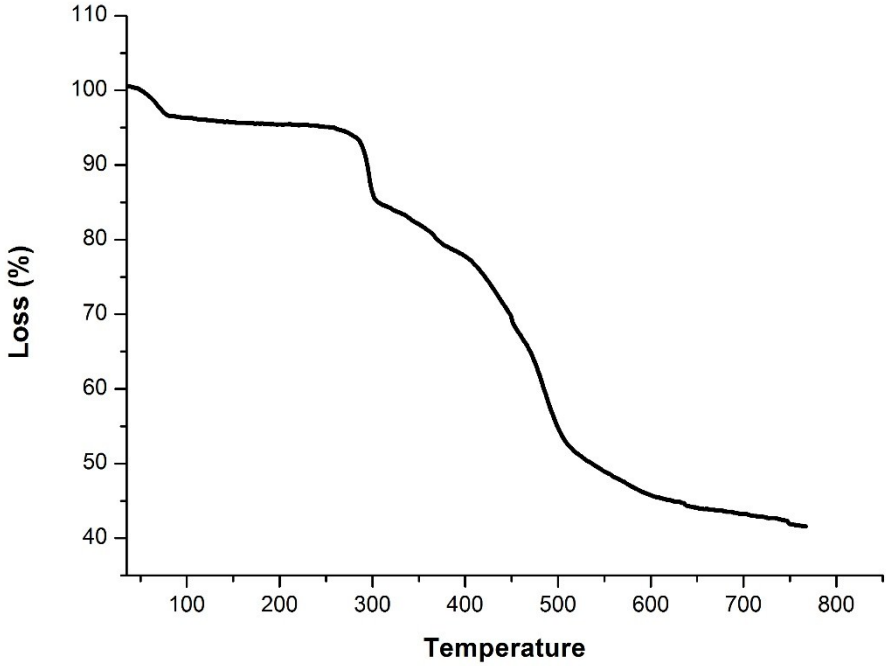

Fig. S3 view of the TGA

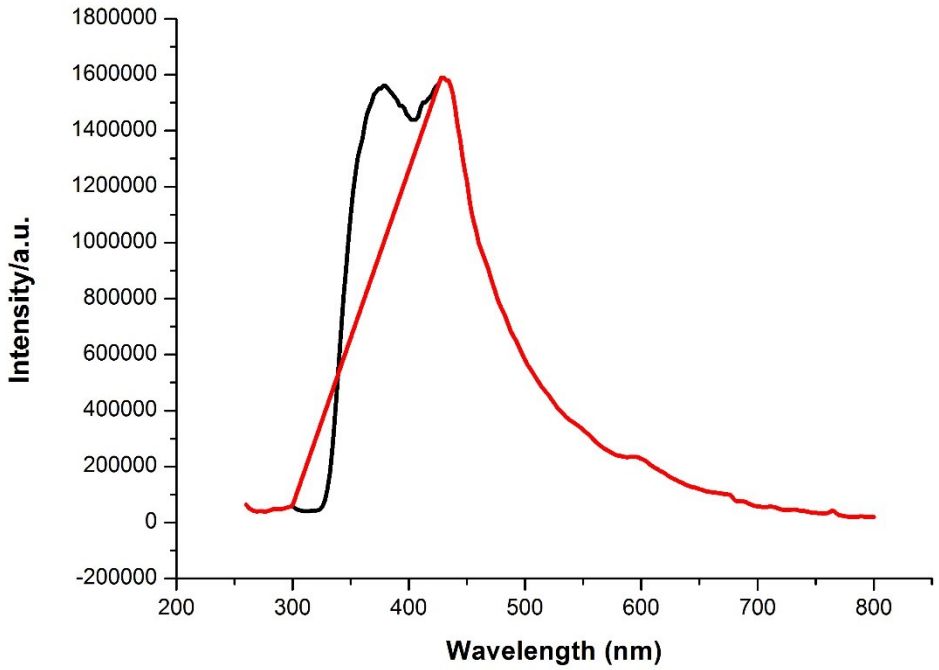

Fig. S4 Solid state excitation (red, λ_{em} = 415 nm) and emission (black, λ_{ex} = 335 nm) spectrum of H_3TZBPDC.

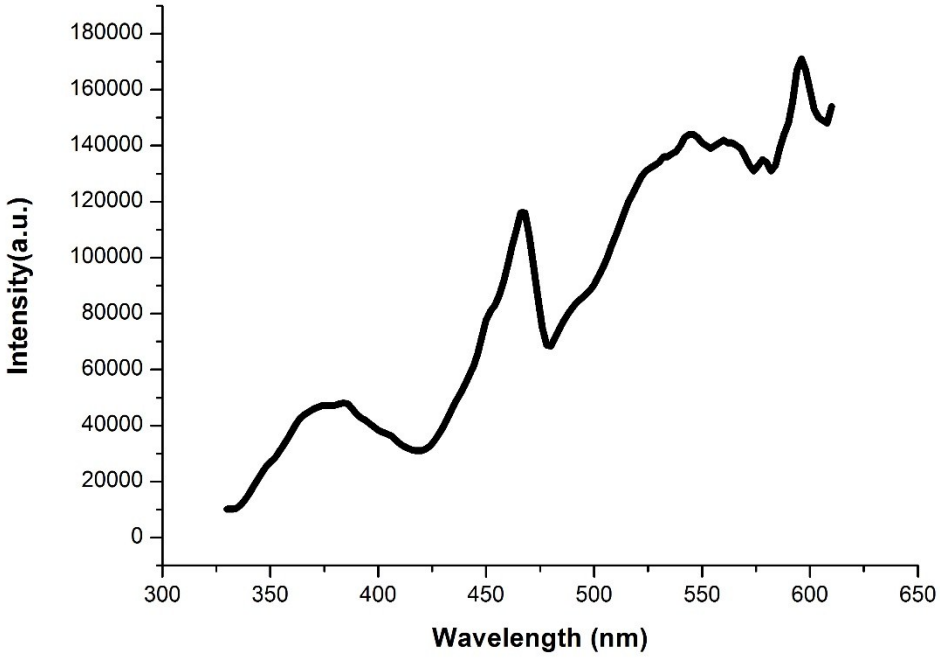

Fig. S5 Solid state excitation spectrum of **1**(λ_{ex} = 310 nm).

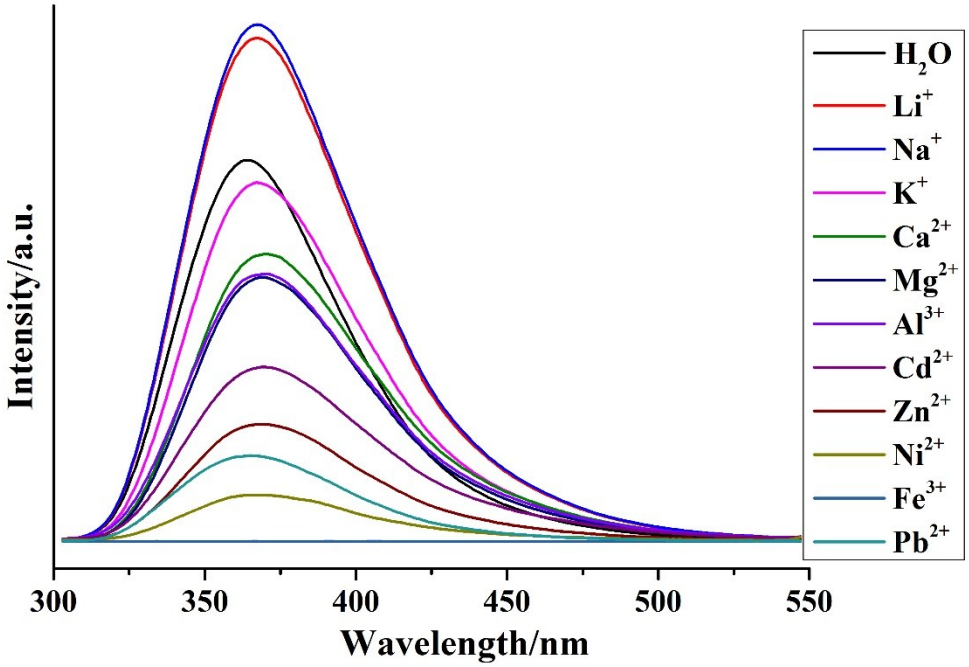

Fig. S6 The photoluminescence intensities spectra of **1** that was dispersed in the solutions of different metal ions.

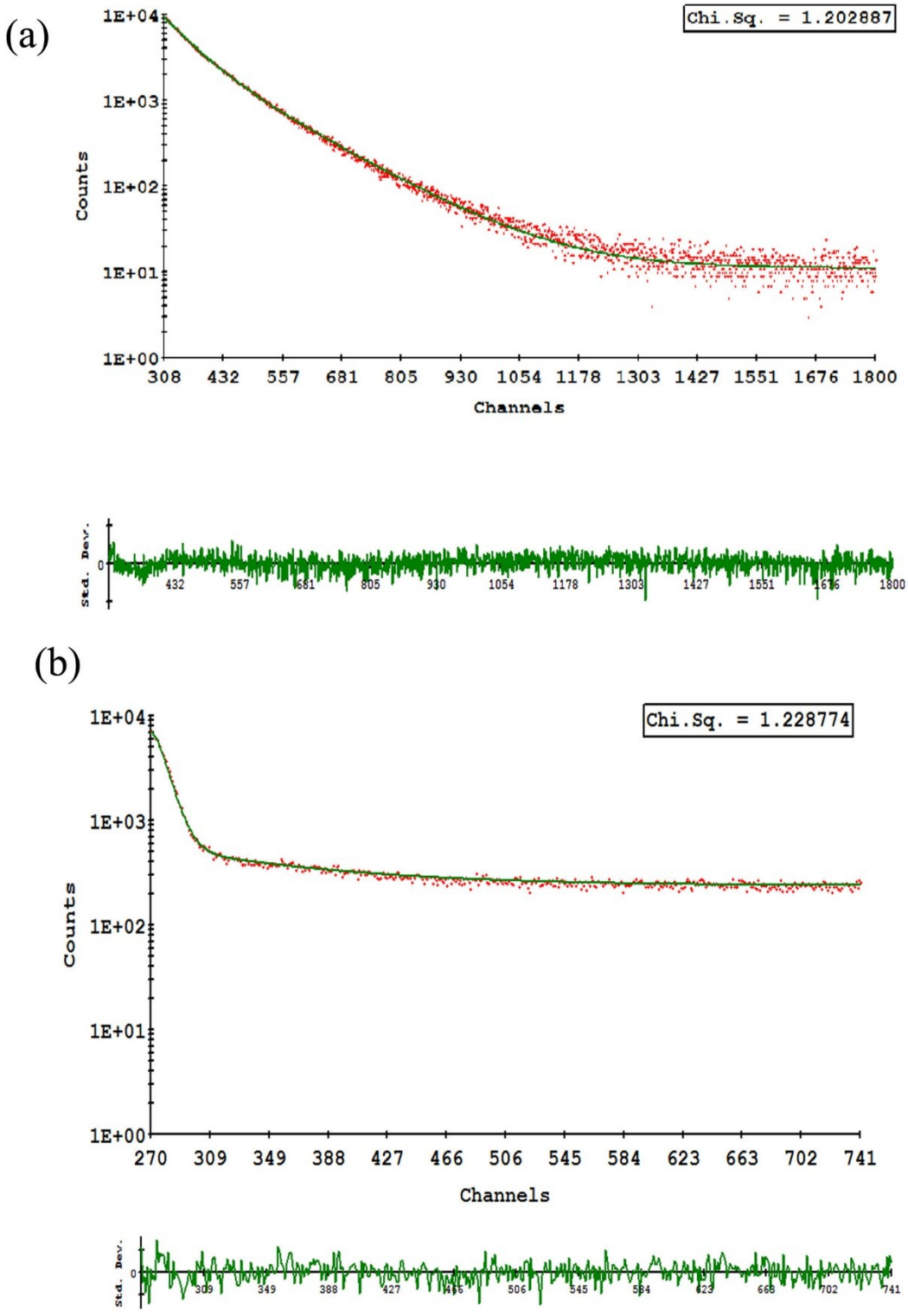

Fig. S7 Comparison of the fluorescence lifetime of **1** (a) and Fe^{3+}@ **1** (b).

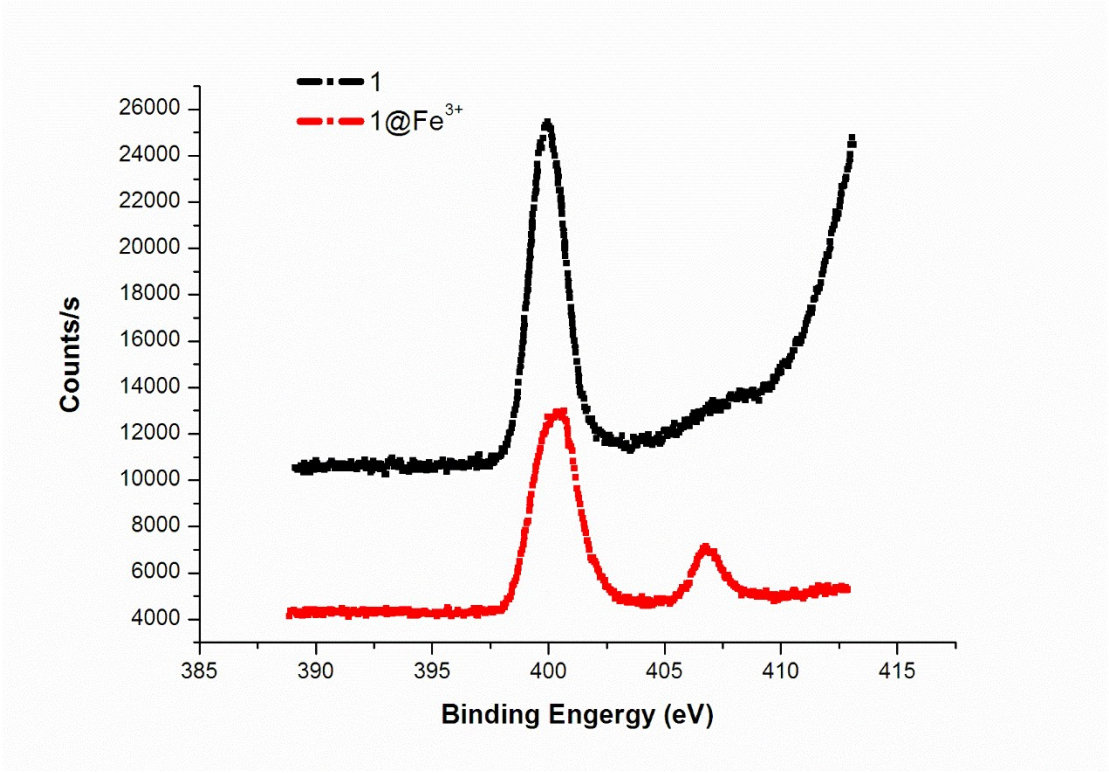

Fig. S8 The N1s XPS spectra of the **1** (black) and **1**@Fe^{3+} (red).

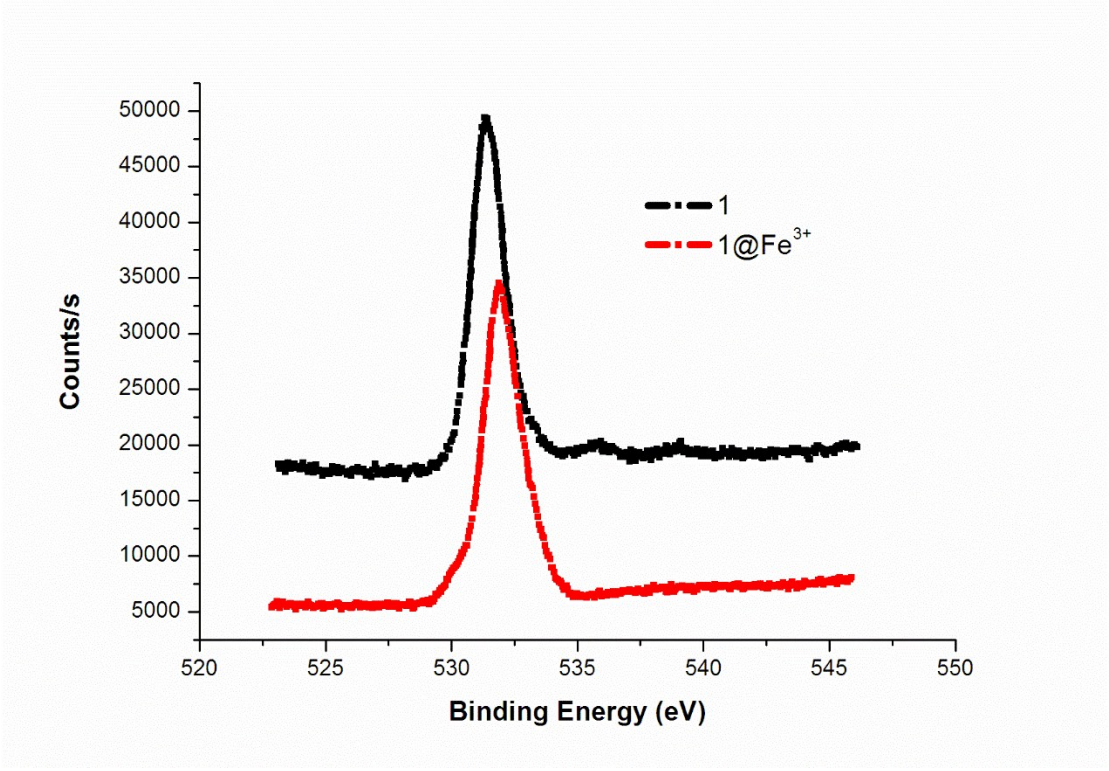

Fig. S9 The O1s XPS spectra of the **1** (black) and **1**@Fe^{3+} (red).

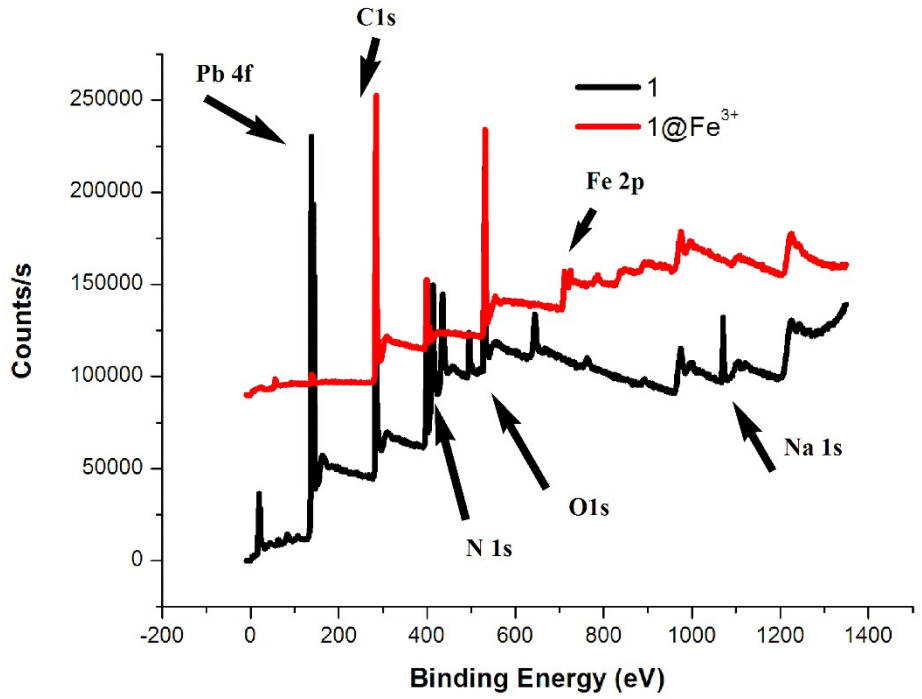

Fig. S10 The XPS spectra of the **1**@Fe^{3+} (red) and **1** (black).

IR spectra

1 was determined in the frequency range of 500–4000 cm^{-1}, as shown in Fig. S11. **1** shows broad bands in the 3500–3100 cm^{-1} region, which may be ascribed to –OH stretching vibrations of the lattice or coordinated water molecules. The strong peaks at 1615 and 1243 cm^{-1} may be attributed to the asymmetric and symmetric vibrations of carboxyl groups. The strong peaks at 1551, 1498, 1435, 1326 cm^{-1} for **1**, suggest the ν_{C-N} stretching vibrations of the triazole rings of the TZBPDC.

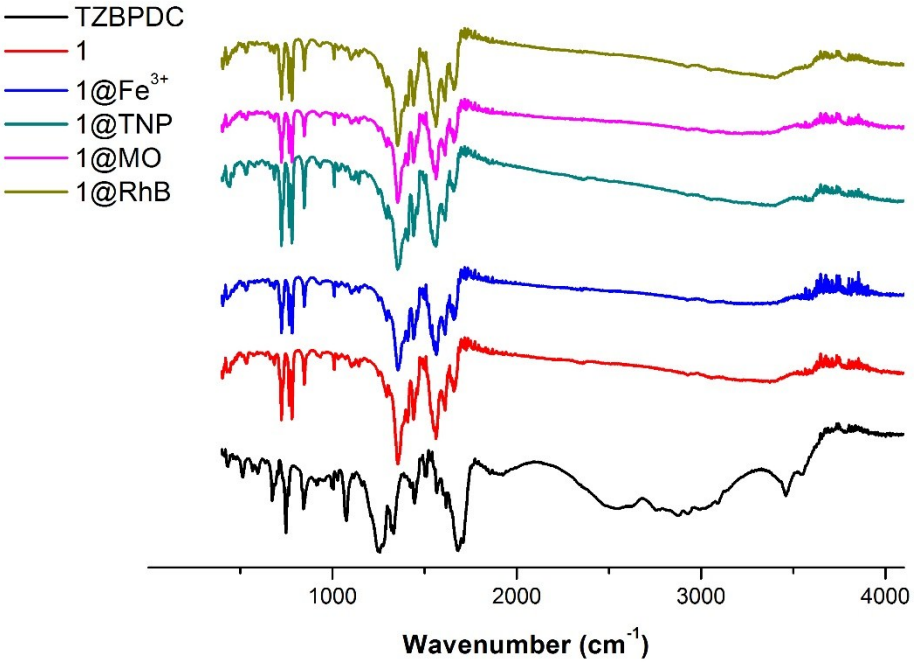

Fig. S11 The IR spectra of **1**, H_2L, **1**@Fe^{3+}, **1**@ACs (ACs = nitro-aromatic and aromatic compounds) and the samples after degradation of dyes.

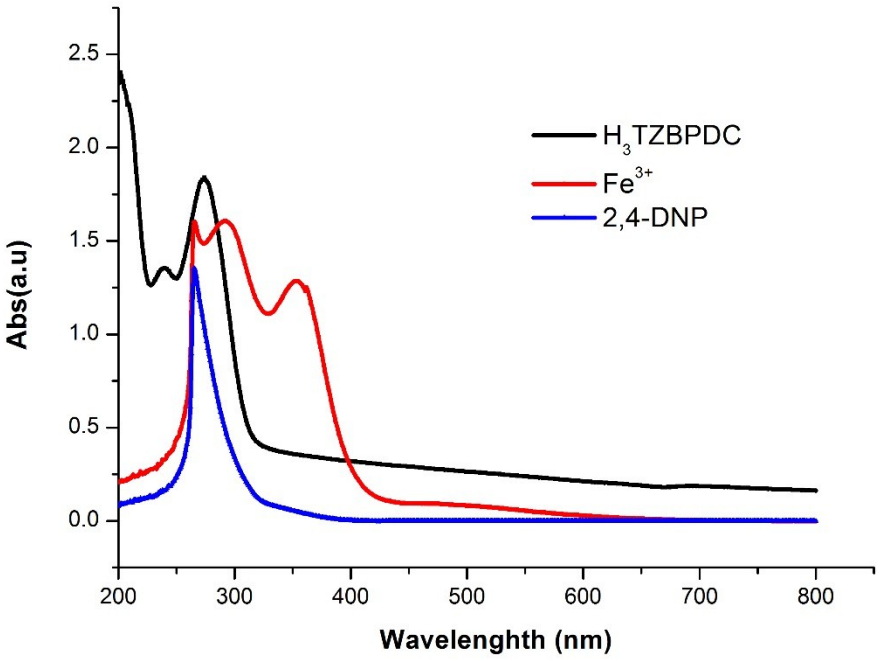

Fig. S12 view of spectra of the UV-vis for different analytes, **1** and ligand.

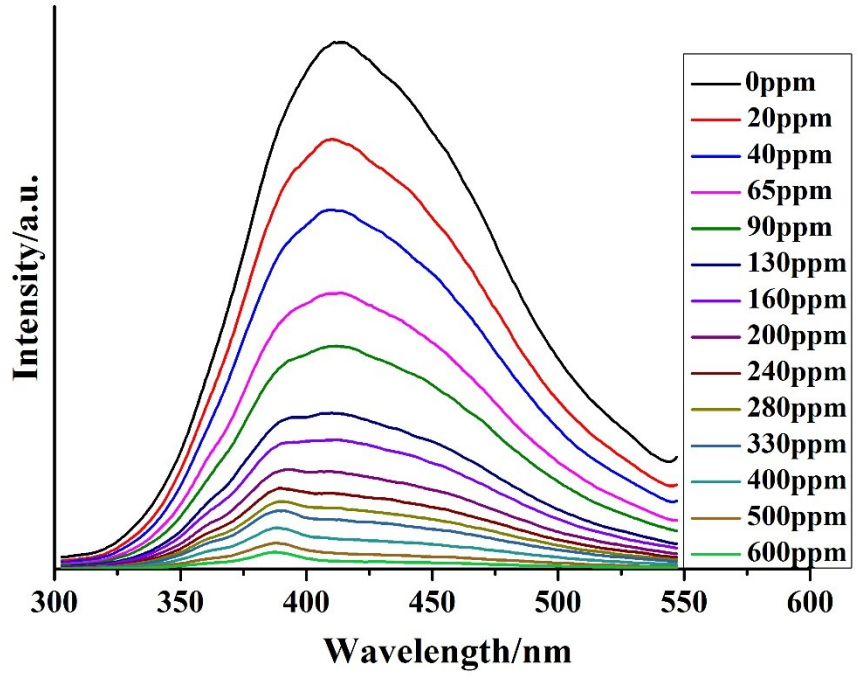

Fig. S13Luminescent quenching of **1** dispersed in ethanol by the gradual addition of 1 mM solution of 1,3-DNB in DMF.

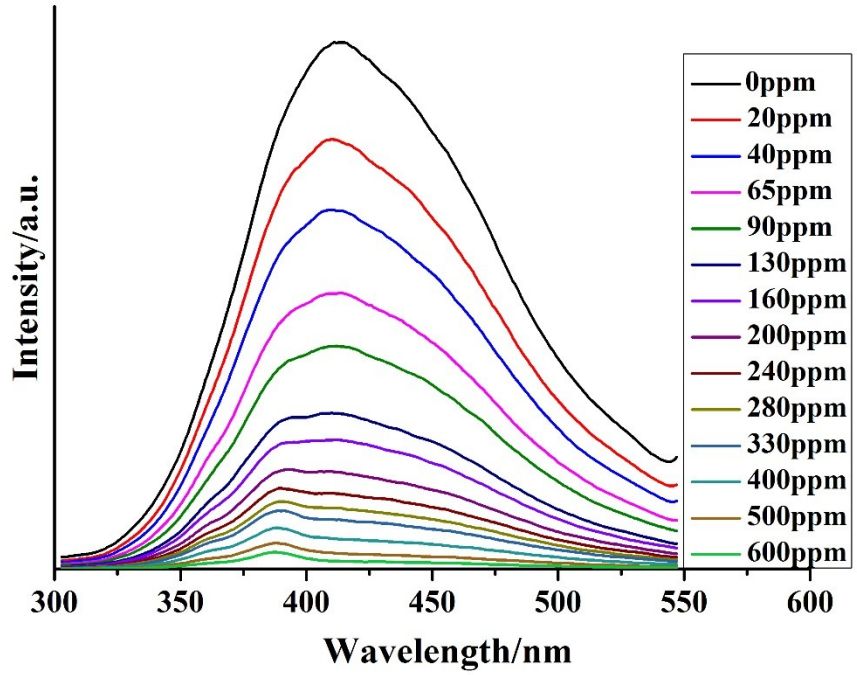

Fig. S14 The Stern–Volmer plot of **1** against 1,3-DNB.

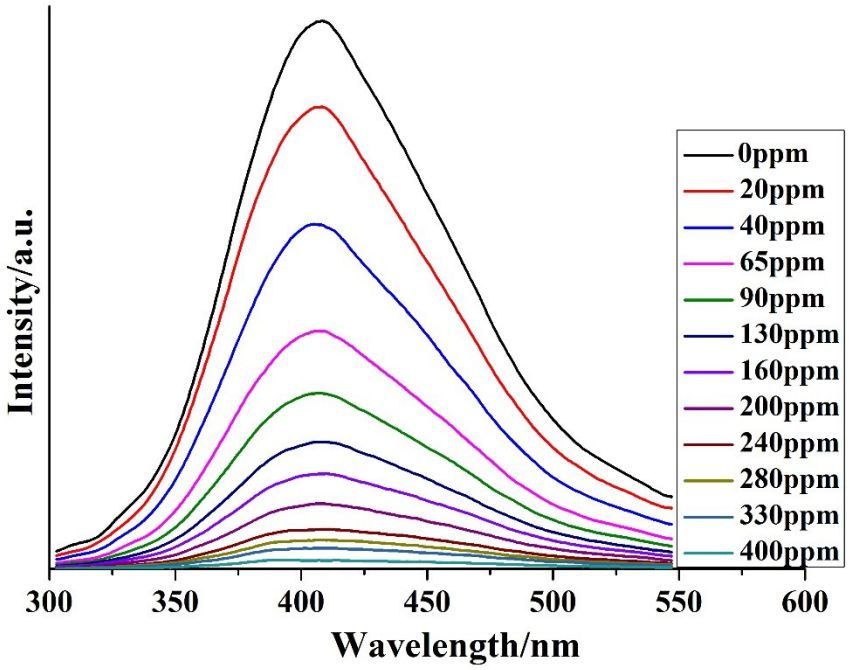

Fig. S15 Luminescent quenching of **1** dispersed in ethanol by the gradual addition of 1 mM solution of 2,4-DNT in DMF.

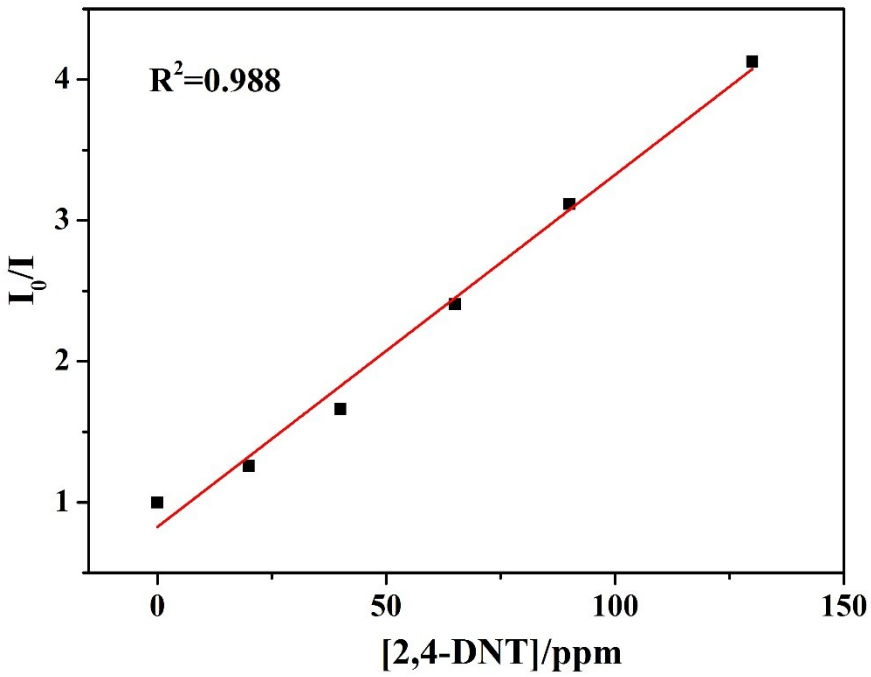

Fig. S16 Stern–Volmer plot for the fluorescence quenching of **1** upon the addition of 2,4-DNT.

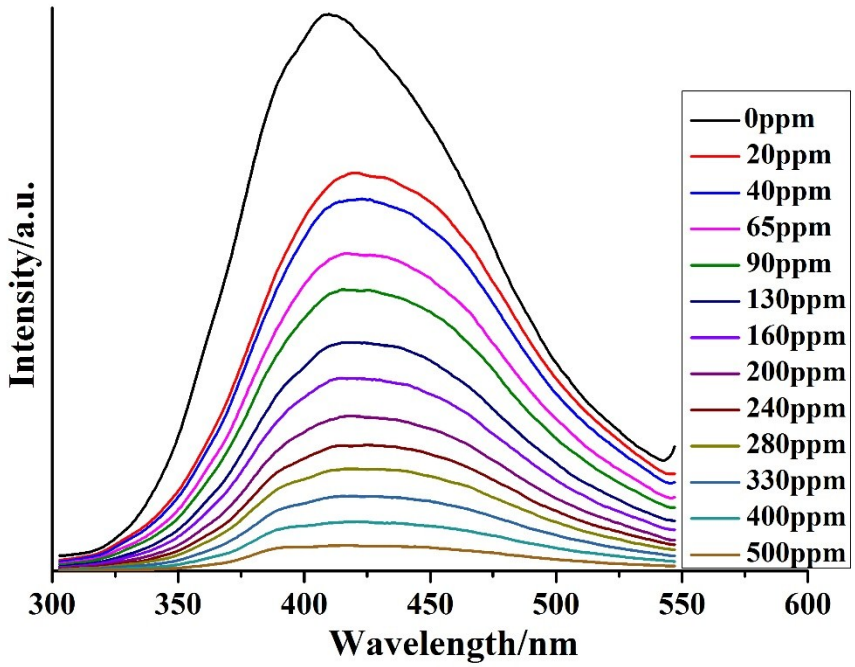

Fig. S17 Luminescent quenching of **1** dispersed in ethanol by the gradual addition of 1 mM solution of 2,6-DNT in DMF.

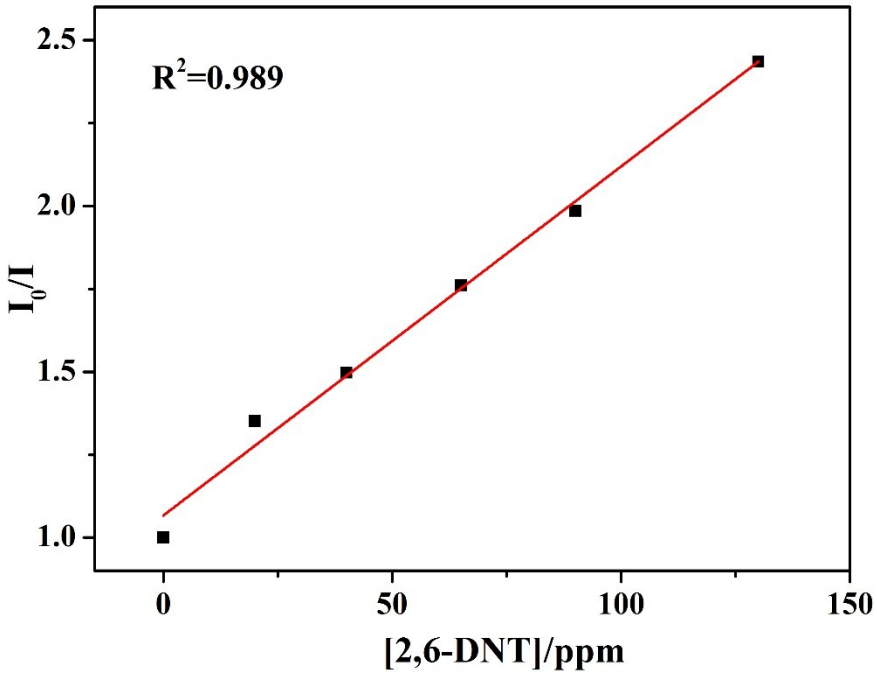

Fig. S18 Stern–Volmer plot for the fluorescence quenching of **1** upon the addition of 2,6-DNT.

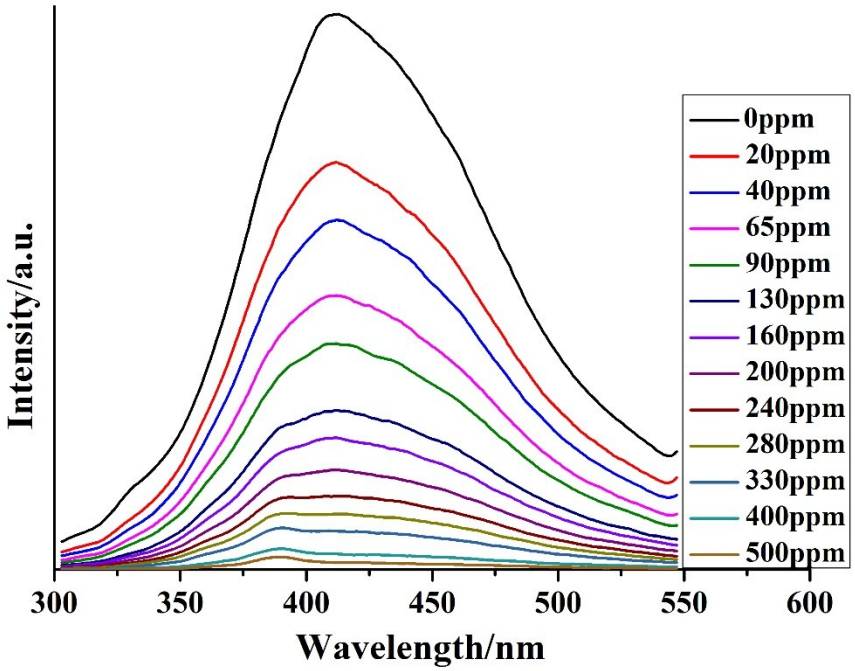

Fig. S19 Luminescent quenching of **1** dispersed in ethanol by the gradual addition of 1 mM solution of 2-NT in DMF.

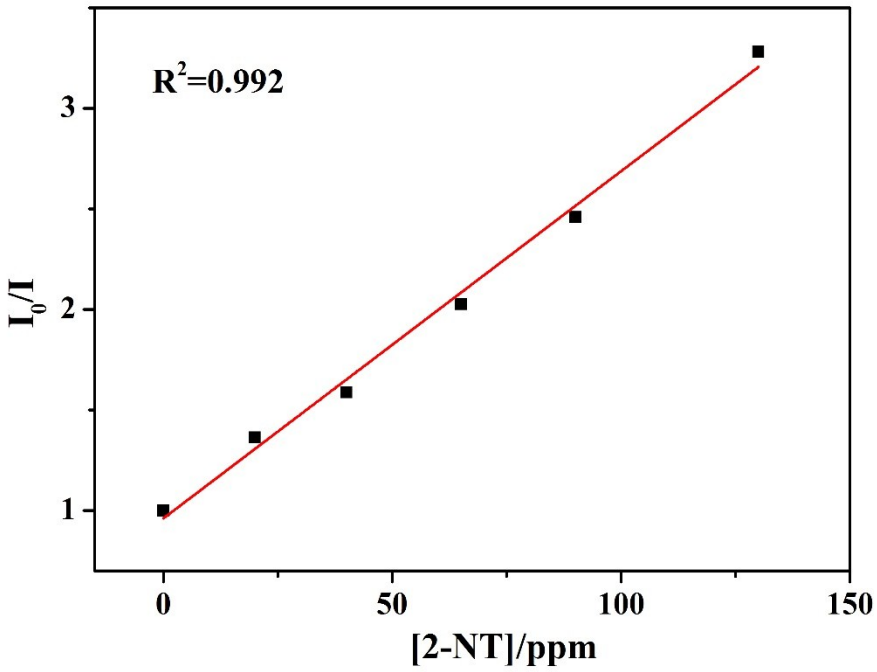

Fig. S20 Stern–Volmer plot for the fluorescence quenching of **1** upon the addition of 2-NT.

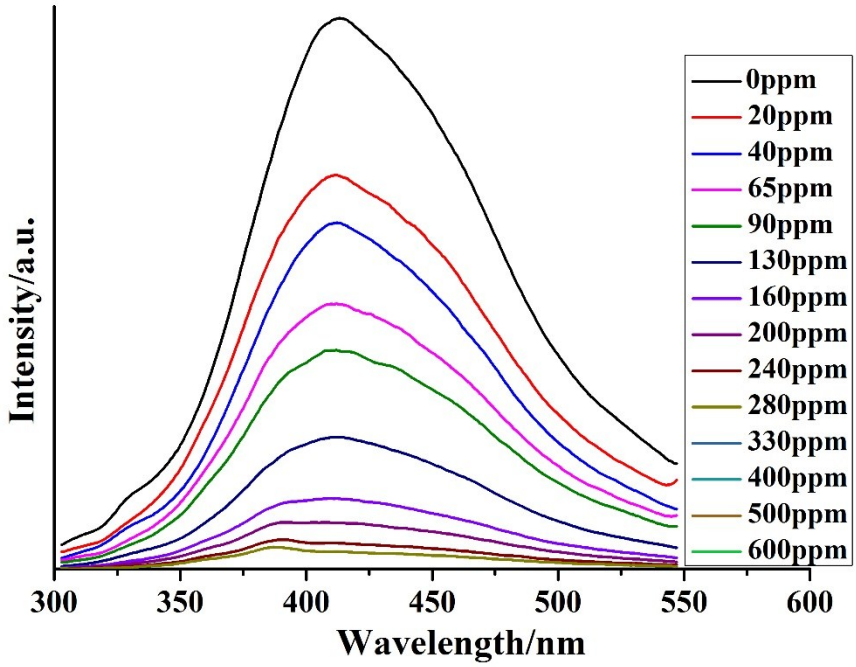

Fig. S21 Luminescent quenching of **1** dispersed in ethanol by the gradual addition of 1 mM solution of 4-NT in DMF.

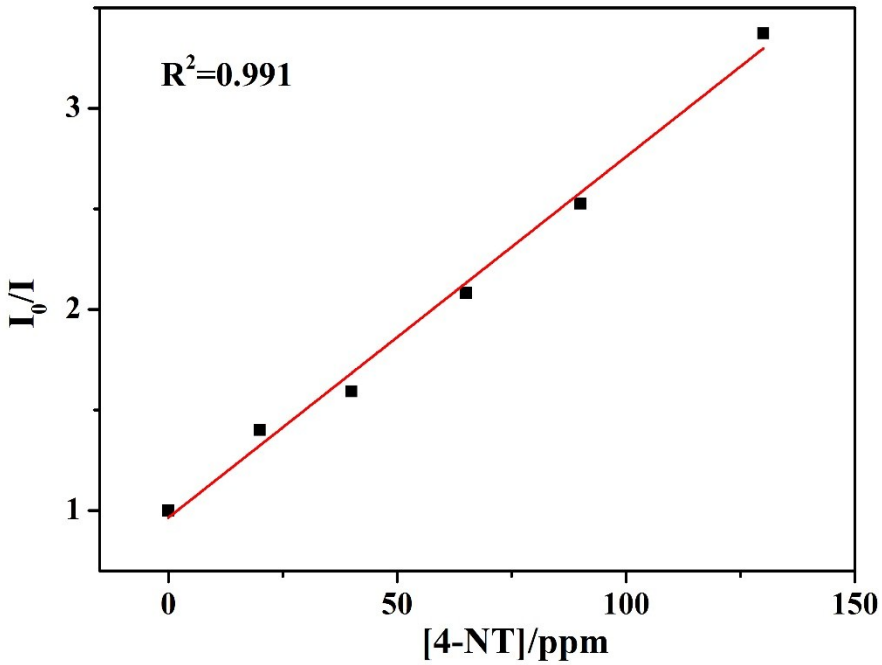

Fig. S22 Stern–Volmer plot for the fluorescence quenching of **1** upon the addition of 4-NT.

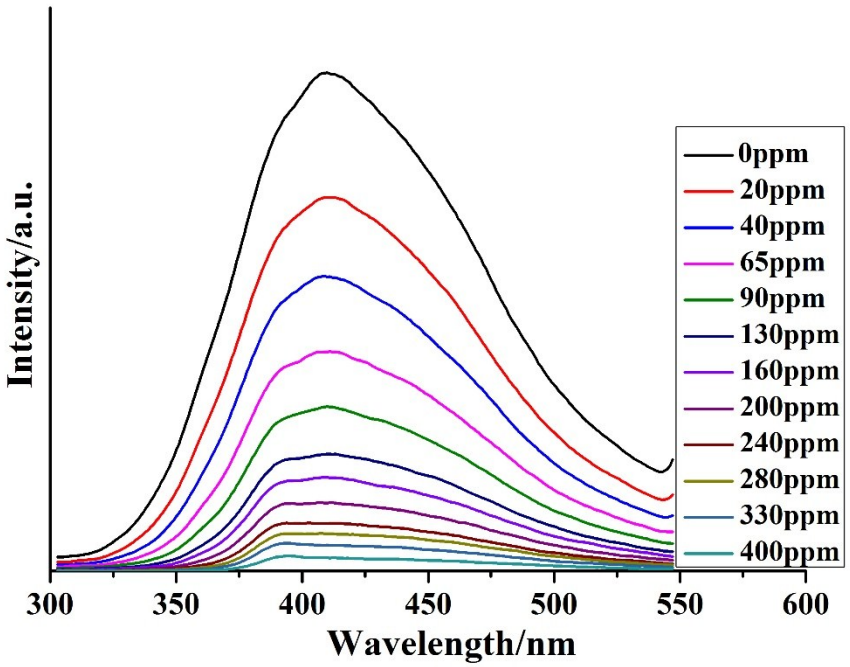

Fig. S23 Luminescent quenching of **1** dispersed in ethanol by the gradual addition of 1 mM solution of MNP in DMF.

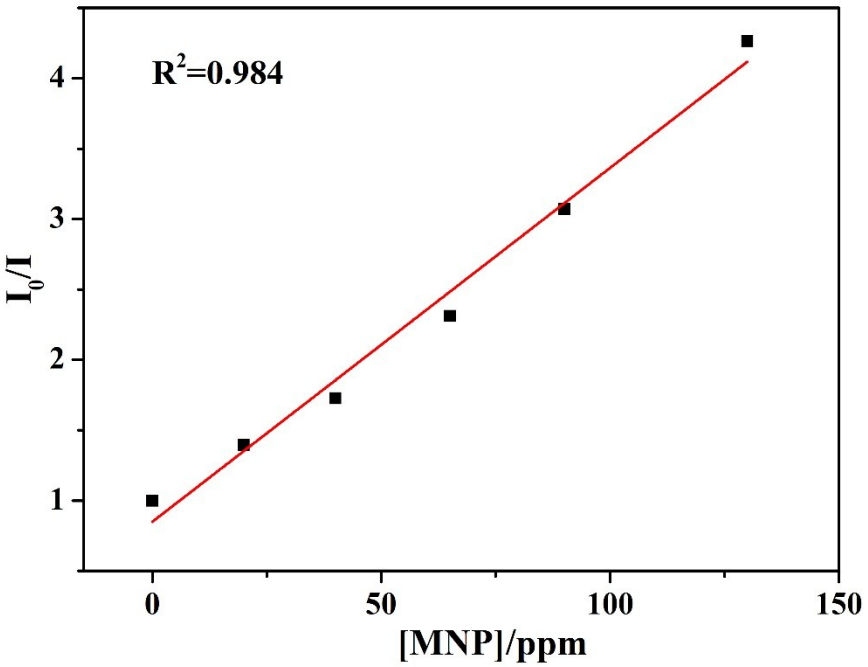

Fig. S24 Stern–Volmer plot for the fluorescence quenching of **1** upon the addition of MNP.

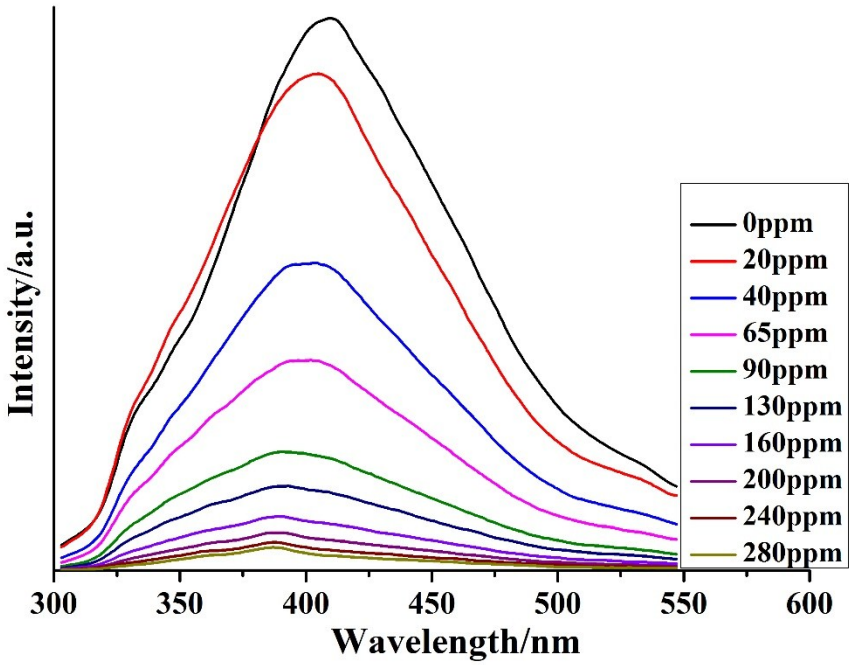

Fig. S25 Luminescent quenching of **1** dispersed in ethanol by the gradual addition of 1 mM solution of NB in DMF.

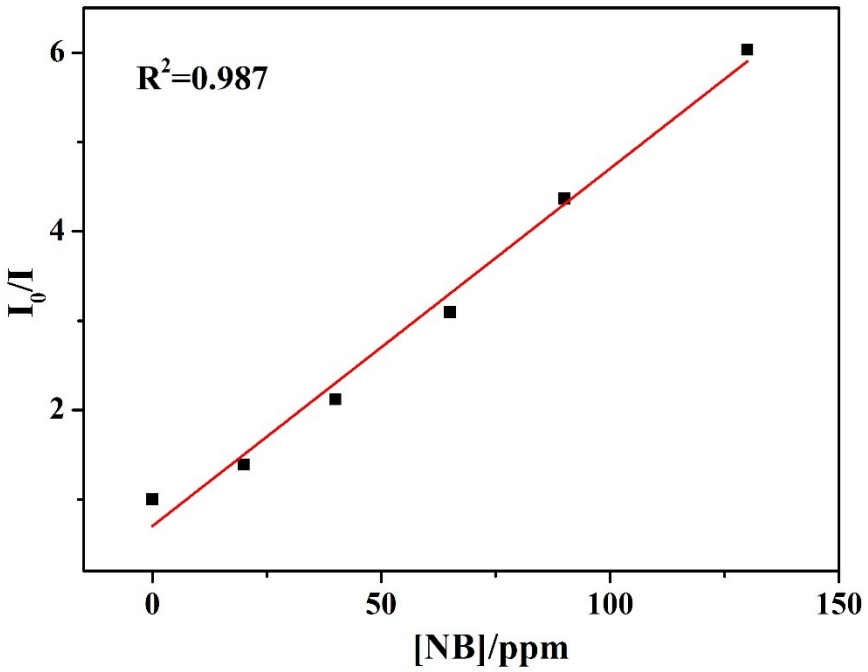

Fig. S26 Stern–Volmer plot for the fluorescence quenching of **1** upon the addition of NB.

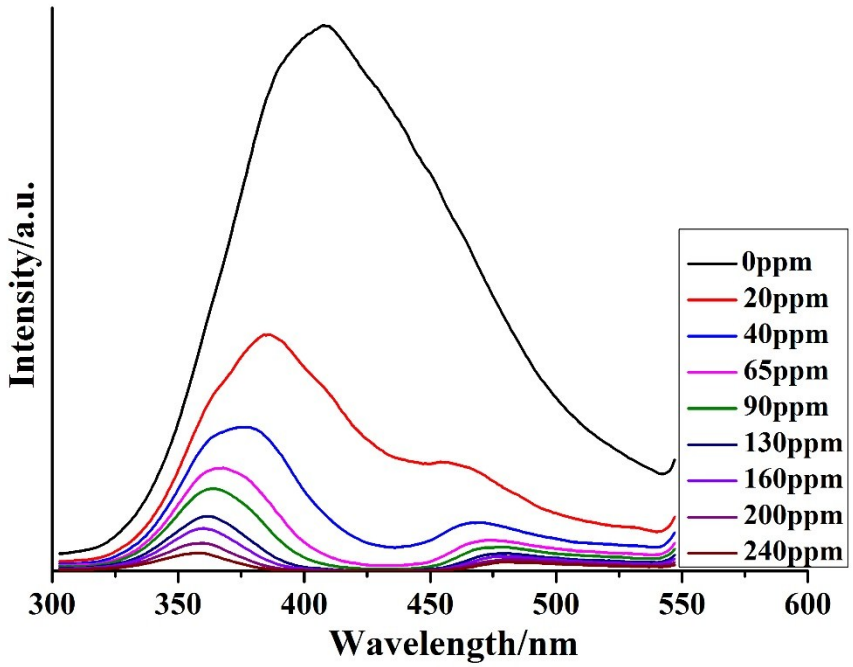

Fig. S27 Luminescent quenching of **1** dispersed in ethanol by the gradual addition of 1 mM solution of PNP in DMF.

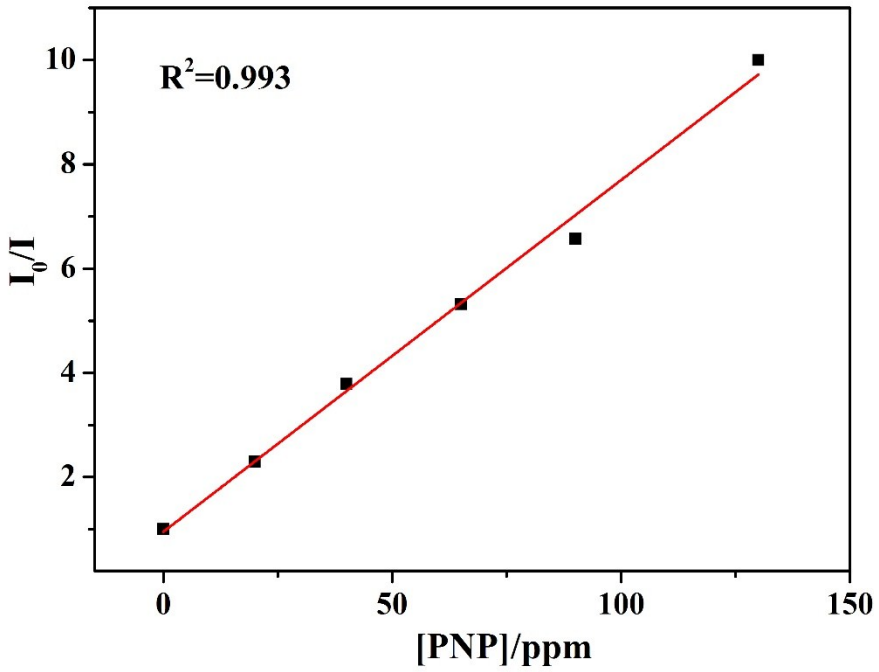

Fig. S28 Stern–Volmer plot for the fluorescence quenching of **1** upon the addition of PNP.

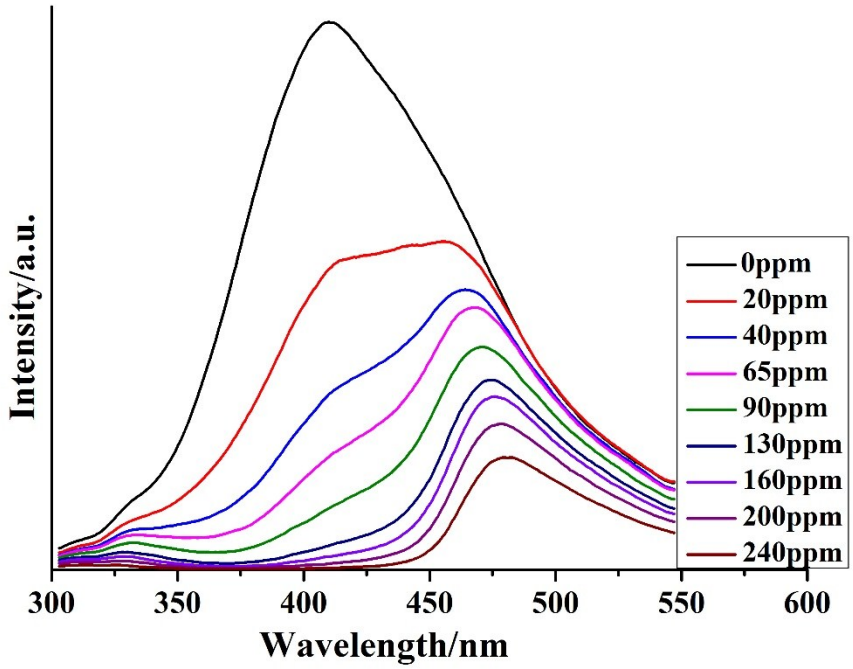

Fig. S29 Luminescent quenching of **1** dispersed in ethanol by the gradual addition of 1 mM solution of TNP in DMF.

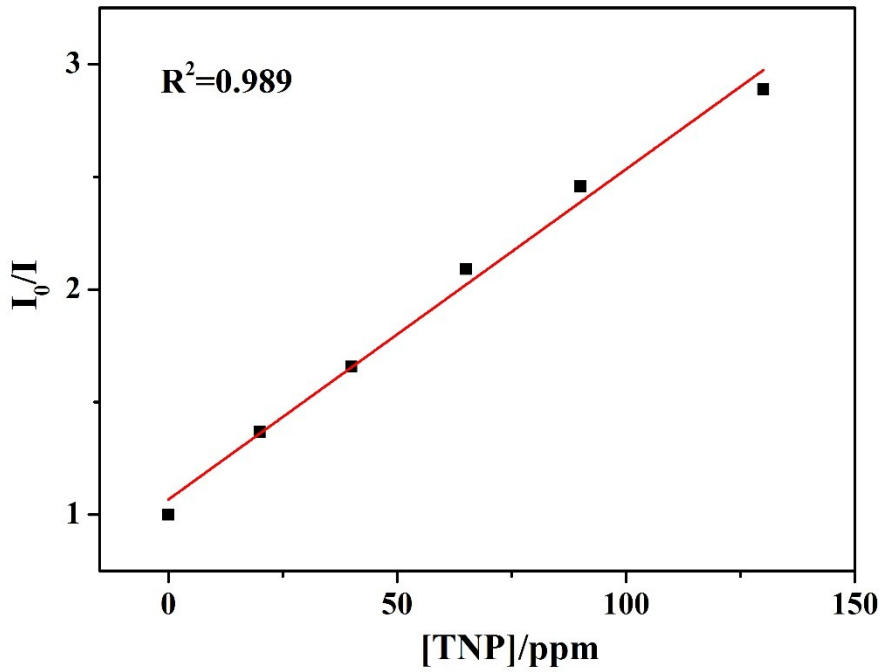

Fig. S30 Stern–Volmer plot for the fluorescence quenching of **1** upon the addition of TNP.

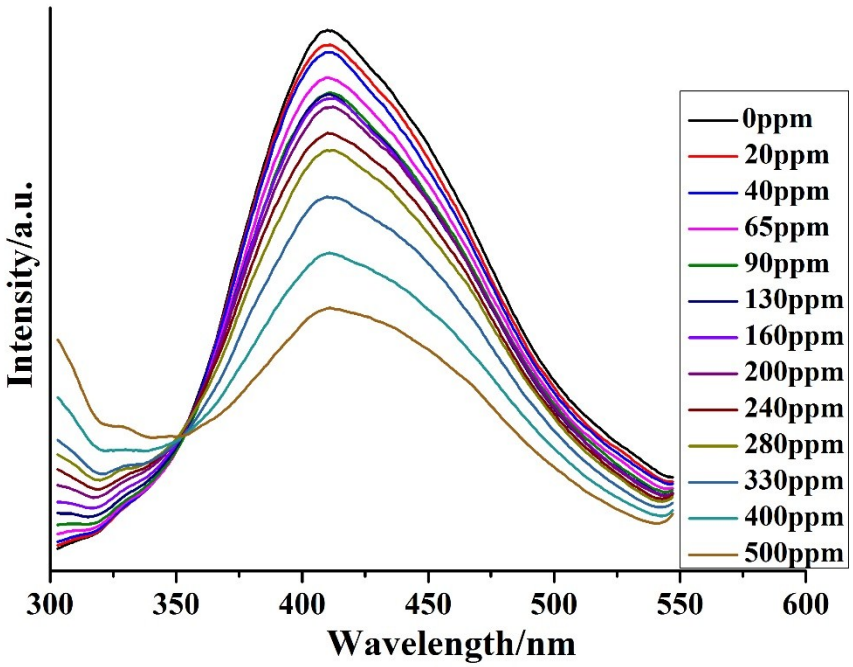

Fig. S31 Luminescent quenching of **1** dispersed in ethanol by the gradual addition of 1 mM solution of 1,2,4-TMB in DMF.

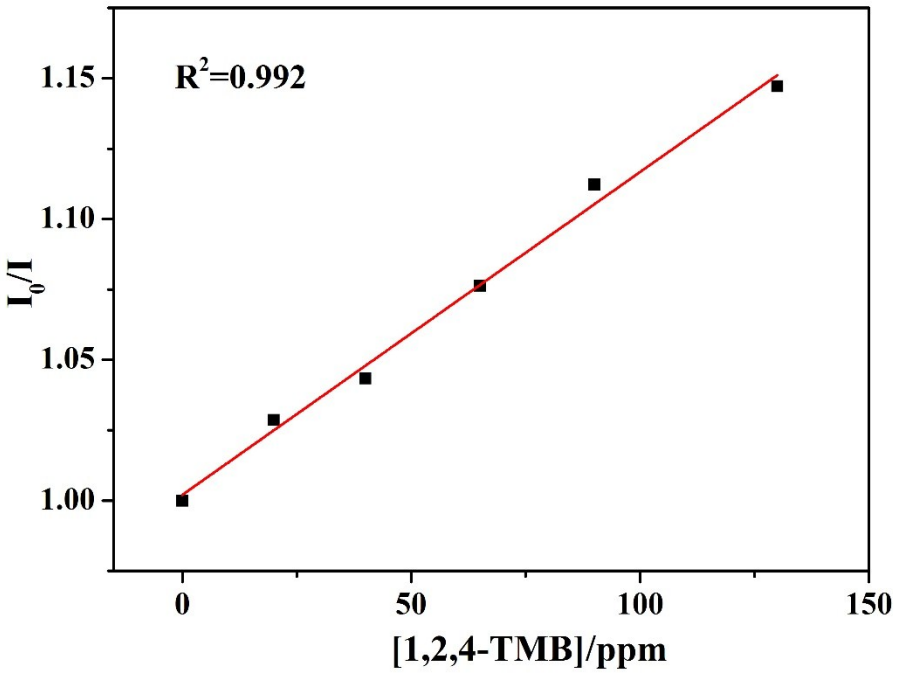

Fig. S32 Stern–Volmer plot for the fluorescence quenching of **1** upon the addition of 1,2,4-TMB.

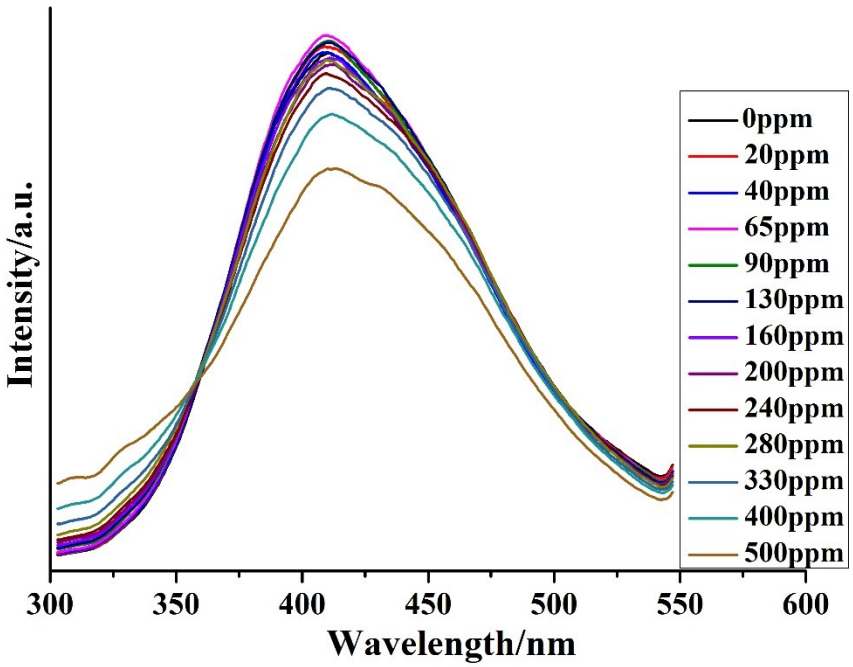

Fig. S33 Luminescent quenching of **1** dispersed in ethanol by the gradual addition of 1 mM solution of 1,3,5-TMB in DMF.

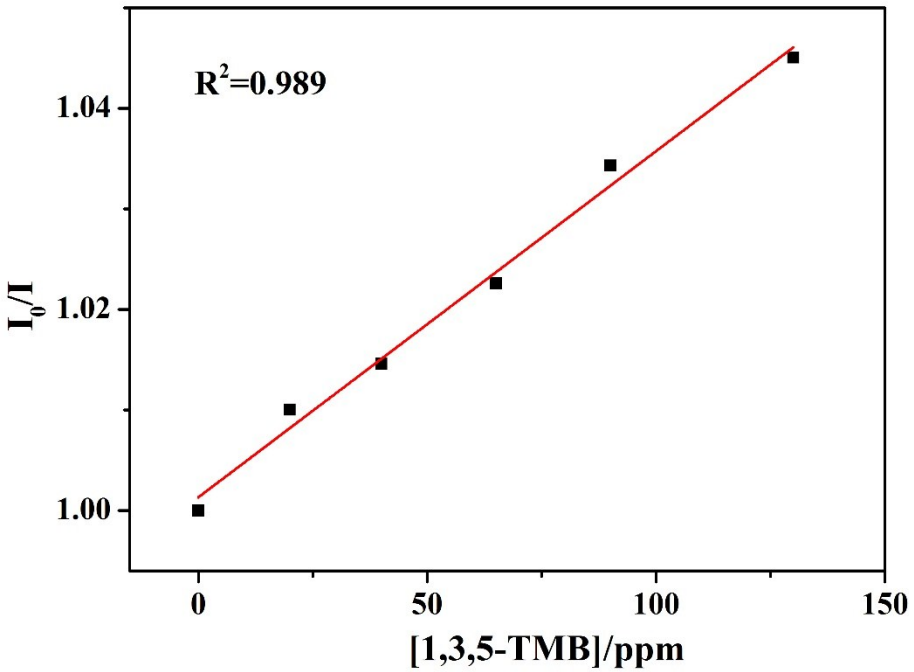

Fig. S34 Stern–Volmer plot for the fluorescence quenching of **1** upon the addition of 1,3,5-TMB.

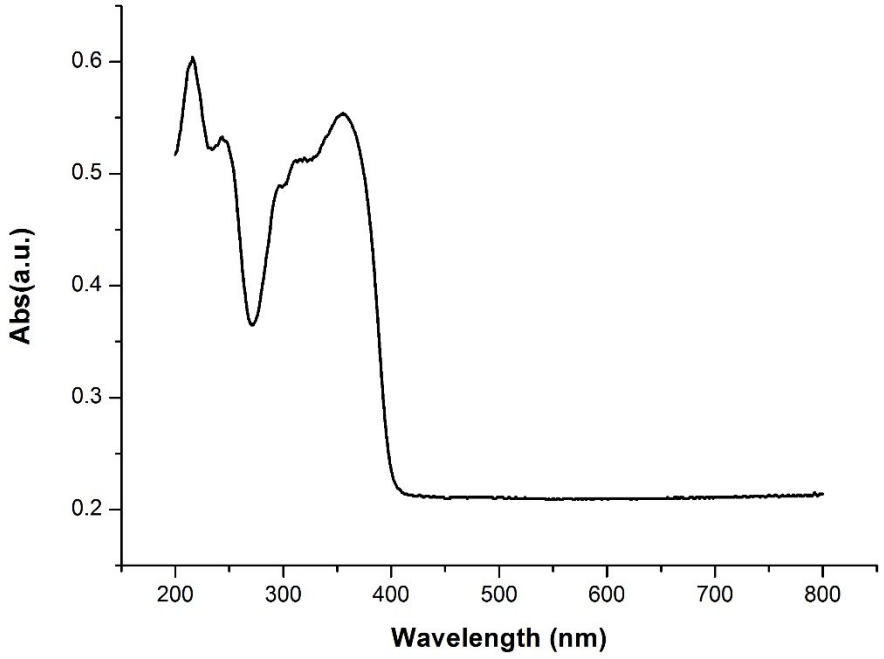

Fig. S35 UV–vis diffuse-reflectance spectra of **1** with $BaSO_4$ as background.

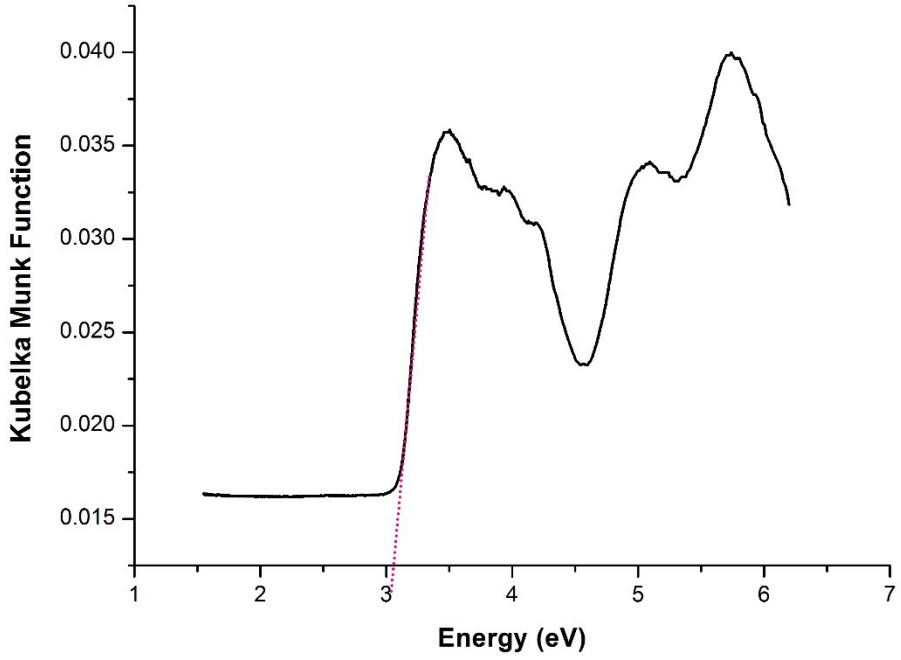

Fig. S36 Solid-state optical diffuse-reflection spectra of **1** derived from diffuse reflectance data at ambient temperature. The intercept of the extrapolated absorption edge on the energy scale (x axis) gives the band gap of the sample.

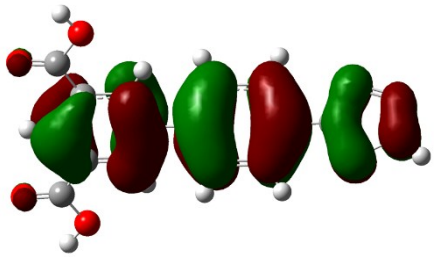 HOMO H_3L	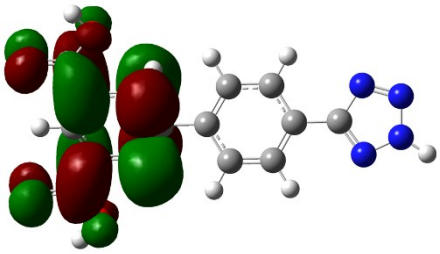 LUMO H_3L
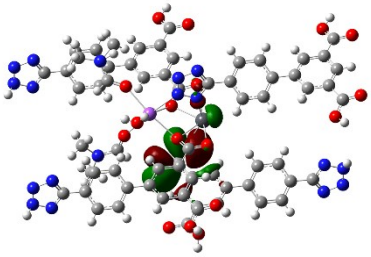 HOMO **1**	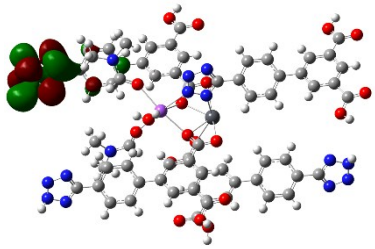 LUMO **1**
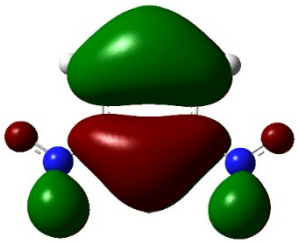 HOMO 1,3-DNB	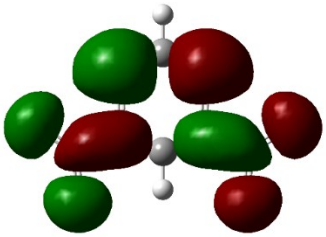 LUMO 1,3-DNB
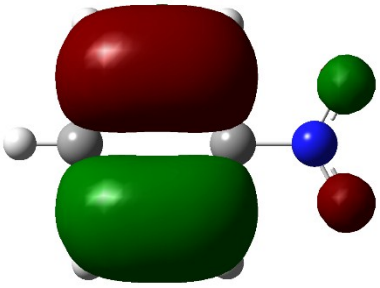 HOMO NB	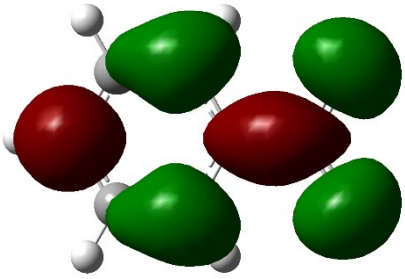 LUMO NB
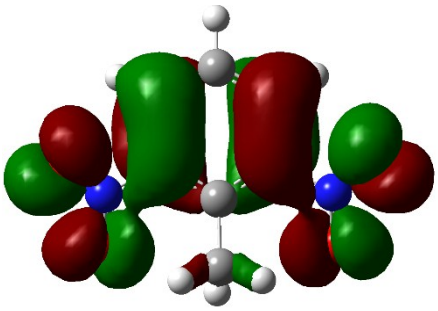 HOMO 2,6-DNT	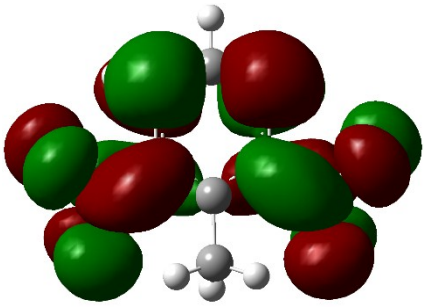 LUMO 2,6-DNT

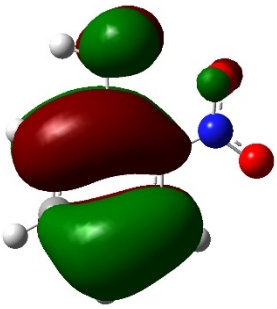 HOMO 2-NT	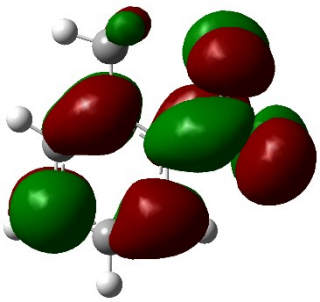 LUMO 2-NT
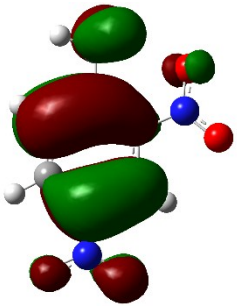 HOMO 2,4-DNT	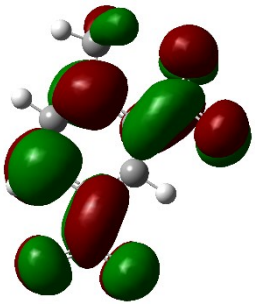 LUMO 2,4-DNT
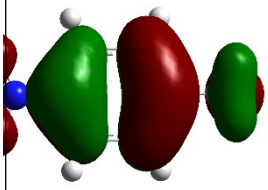 HOMO 4-NT	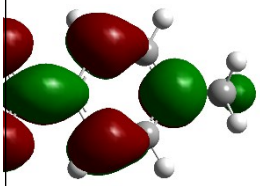 LUMO 4-NT
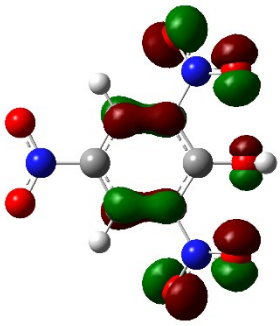 HOMO TNP	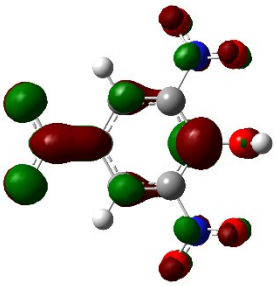 LUMO TNP

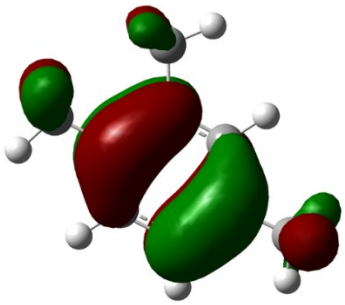 HOMO 1,2,4-TMB	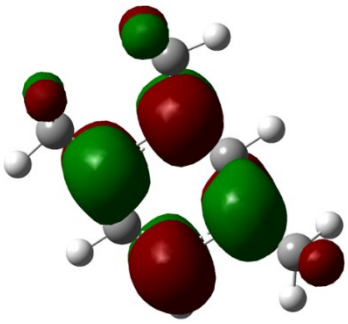 LUMO 1,2,4-TMB
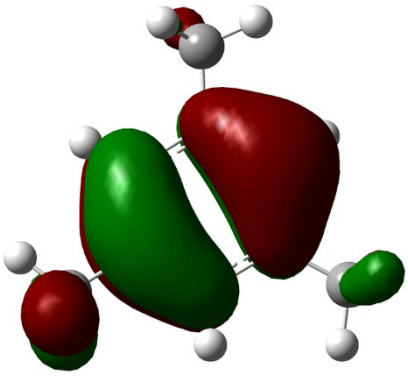 HOMO 1,3,5-TMB	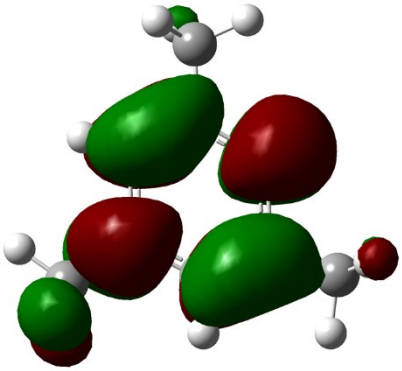 LUMO 1,3,5-TMB
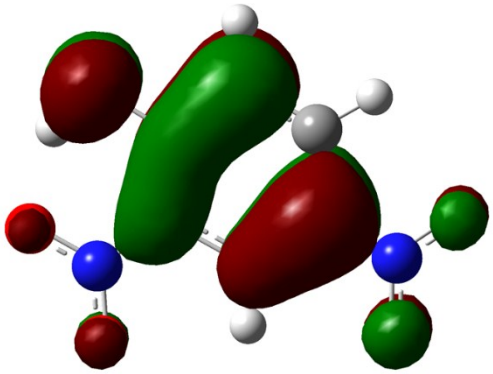 HOMO 2,4-DNP	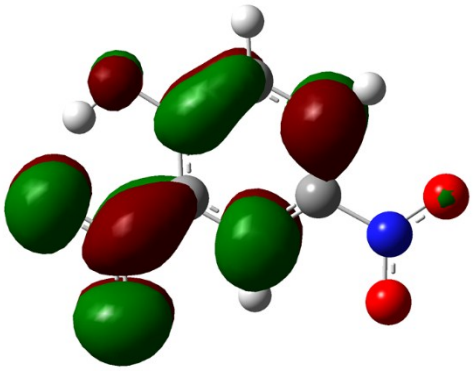 LUMO 2,4-DNP
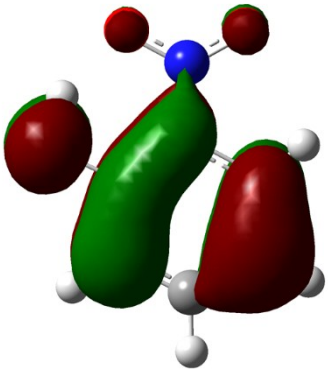 HOMO o-nitro phenol	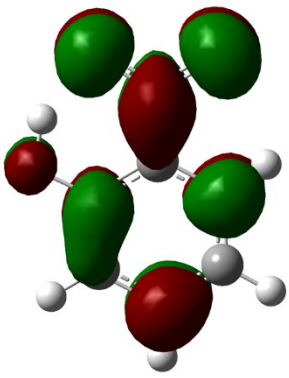 LUMO o-nitro phenol

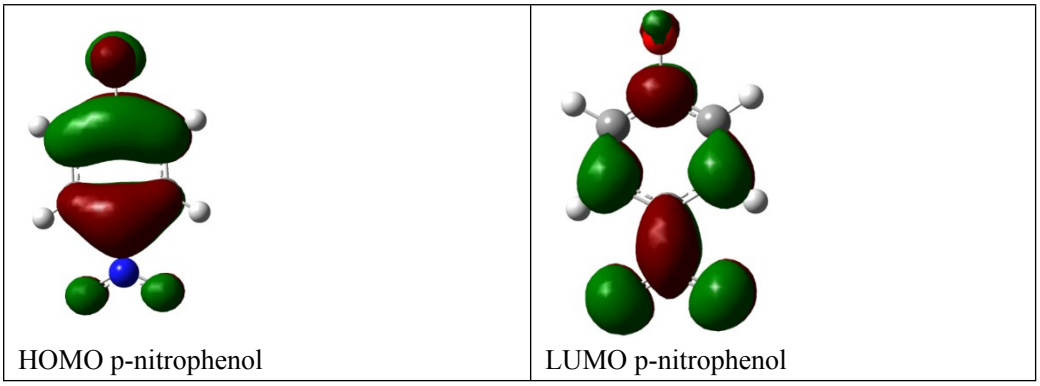

Fig. S37 HOMO–LUMO energies of the NACs along with CP **1** and H_3L.

Table S1. Crystal data and structure refinement information for **1**

Compound	**1**
Formula	$C_{21}H_{23}N_6NaO_7Pb$
Crystal system	triclinic
Space group	*P-1*
Crystal color	colorless
a, [Å]	10.0155(3)
b, [Å]	11.6906(3)
c, [Å]	11.8211(4)
α, [°]	97.673(2)
β, [°]	99.525(1)
γ, [°]	112.778(1)
V, Å ^{3}	1228.49(6)
Z	2
ρ_{calcd}, g/cm^3	1.897
μ, mm^{-1}	6.938
F(000)	680
θ Range, deg	2.27-26.12
Reflection collected	18120/ 0.0671
Goodness-of-fit on F^2	1.012
R_1, $wR_2(I> 2\sigma(I))^*$	0.0352, 0.0643

R_1, wR_2 (all data)**	0.0539, 0.0694

* $R = \sum(F_o - F_c)/\sum(F_o)$, ** $wR_2 = \{\sum[w(F_o^2 - F_c^2)^2]/\sum(F_o^2)^2\}^{1/2}$.

Table S2. Selected bond distances (Å) and angles (°) of **1**

1

Pb(1)-O(4)	2.361(4)	Pb(1)-O(1)#1	2.400(3)
Pb(1)-N(1)	2.418(5)	Pb(1)-O(2)	2.613(3)
Pb(1)-O(3)	2.648(4)	Na(1)-O(1W)	2.327(5)
Na(1)-O(6)	2.381(7)	Na(1)-O(5)	2.406(7)
Na(1)-O(4)	2.460(4)	Na(1)-N(2)	2.497(5)
O(2)-Pb(1)-O(4)	123.24(12)	Na(1)-Pb(1)-O(1)	146.22(12)
N(1)-Pb(1)-O(4)	80.24(14)	O(1)-Pb(1)-O(3)	125.06(12)

Symmetric code: -x, -y, -z.

Table S3 Comparison of the selected materials in detective sensitivity for Fe^{3+} ions

Material	Sensitivity	Reference
$Eu(acac)_3@Zn(C_{15}H_{12}NO_2)_2$	5×10^{-3} M	1
$Eu(C_{33}H_{24}O_{12})(H_2NMe)(H_2O)$	2×10^{-4} M	2
$Eu(C_{22}H_{14}O_2)_3$	10^{-4} M	3
$[Eu(BTPCA)(H_2O)]\cdot2DMF\cdot3H_2O$	10^{-5} M	4
MIL-53(Al)	0.9×10^{-6} M	5
$\{[LnCd_2(DTPA)_2(H_2O)_4]\cdot4H_2O$	1.5×10^{-5} M	6
carbon nanoparticles (CNPs)	0.32×10^{-6} M	7
Fluorescent Gold Nanoclusters	5.4×10^{-6} M	8
$[Cd_3(dpa)(DMF)_2(H_2O)_3]\cdot DMF$	1.75×10^{-4} M	9
$Zn_3L_3(DMF)_2$	10^{-5} M	10
$[[Eu_2(MFDA)_2(HCOO)_2(H_2O)_6]\cdot H_2O$	1.0×10^{-4} M	11
$[Tb_4(OH)_4(DSOA)_2(H_2O)_8]\cdot(H_2O)_8$	10^{-6} M	12
$[H_2N(Me)_2][Eu_3(OH)(bpt)_3(H_2O)_3](DMF)_2\cdot(H_2O)_4$	10^{-5} M	13
$[Eu_2(MFDA)_2(HCOO)_2(H_2O)_6]\cdot H_2O$	10^{-5} M	14
TbL	10^{-6} M	15
$[Eu(HL)(H_2O_2)]\cdot2H_2O$	3.0×10^{-4} M	16
1	2.1×10^{-5} M	*In this work*

References:

[1] G. G. Hou, Y. Liu, Q. K. Liu, J. P. Ma and Y. B. Dong, *Chem. Commun.*2011, ***47***, 10731-10733.
[2] S. Dang, E. Ma, Z.M. Sun and H. J. Zhang, *J. Mater. Chem.* 2012, ***22***, 16920-16926.
[3] M. Zheng, H. Q. Tan, Z. G. Xie, L. G. Zhang, X. B. Jing and Z. C. Sun, *ACS Appl. Mater. Interfaces,* 2013, ***5***, 1078-1083.
[4] Q. Tang, S. X. Liu, Y. W. Liu, J. Miao, S. J. Li, L. Zhang, Z. Shi and Z. P. Zheng, *Inorg. Chem.*2013, ***52***, 2799-2801.
[5] C. X. Yang, H. B. Ren and X. P. Yan, *Anal. Chem.*2013, ***85***, 7441-7446.
[6] Q. Liu, F. Wan, L. X. Qiu, Y. Q. Sun and Y. P. Chen, *RSC Adv*., 2014, ***4***, 27013-27021.
[7] K. G. Qu, J. S. Wang, J. S. Ren and X. G. Qu, *Chem. Eur. J.* 2013, ***19***, 7243-7249.
[8] J.-A. A. Ho, H.-C. Chang and W.-T. Su, *Anal. Chem*. 2012, ***84***, 3246-3253.
[9] J. C. Jin, L. Y. Pang, G. P. Yang, L. Hou and Y. Y. Wang, *Dalton Trans*., 2015, ***44***, 17222–17228.
[10] Z. C. Yu, F. Q. Wang, X. Y. Lin, C. M. Wang, Y. Y. Fu, X. J. Wang, Y. N. Zhao and G. D. Li, *J. Solid. State. Chem*., 2015, ***232***, 96-101.
[11] X. H. Zhou, L. Li, H. H. Li, T. Yang and W. Huang, *Dalton Trans*., 2013, **42**, 12403–12409.
[12] X. Y. Dong, R. Wang, J. Z. Wang, S. Q. Zang and T. C. W. Mak, *J. Mater. Chem*. A, 2015, ***3***, 641–647.
[13] S. Xing, Q. Bing, L. Song, G. Li, J. Liu, Z. Shi, S. Feng and R. Xu, *Chem. – Eur. J.*, 2016, **22**, 16230-16235.
[14] X. Zhou, L. Li, H. Li, A. Li, T. Yang and W. Huang, *Dalton Trans.,* 2013, **42**, 12403-12409.
[15] S. Dang, T. Wang, F. Yi, Q. Liu, W. Yang and Z. Sun, *Chem. – Asian J.*, 2015, **10**, 1703-1709.
[16] Y. Liang, G. Yang, B. Liu, Y. Yan, Z. Xi and Y. Wang, *Dalton Trans.,* 2015, **44**, 13325-13330.